MolMod Connect
2025, Vol. 1, Cite as: doi:10.x/journal.x.x.x

SCIFINITI PUBLISHING

OPEN ACCESS

Research Article

The impact of toxic effector molecule TagX on the amino acid conformation of the Hcp1 monohexameric ring in *Acinetobacter baumannii* type VI secretion system utilizing bioinformatics tools and an AI system

Mohammad Reza Shakibaie*[1,2,3], Samane Shakibaie[4]

[1] Department of Microbiology and Virology,
[2] Medical Informatics Research Center,
[3] Research Center of Tropical and Infectious Diseases, Kerman University of Medical Sciences, Kerman, Iran.
[4] Medical Mycology and Bacteriology Research Center, Kerman University of Medical Sciences, Kerman, Iran.

***Corresponding address:** Professor Mohammad Reza Shakibaie, Kerman University of Medical Sciences, Afzalipour School of Medicine, Kerman, Iran Postal Code: 7616913555 Tel/fax: +983433257665

E-mail: mr_shakibaei@kmu.ac.ir / mohammadreza.shakibaie@gmail.com; samaneshakibaie@gmail.com.

ORCID: https://orcid.org/0000-0003-2524-125X Mohammad Reza Shakibaie

ORCID: https://orcid.org/0000-0002-1517-4551 Samane Shakibaie

ABSTRACT

Limited information is currently available regarding the contraction mechanism of the Hcp-1 hemolysin-coregulated protein within the type VI secretion system (T6SS) of *Acinetobacter baumannii*, particularly about the secretion of toxic effectors. This research aimed to evaluate the mechanism underlying the contraction of the Hcp1 nanotube in response to the putative toxic effector TagX protein by employing bioinformatics tools and artificial intelligence (AI) DeepMind system. To achieve this goal, the amino acid sequence of Hcp1 from *A. baumannii* was retrieved from the GenBank database under accession no. WP_000653195.1 and its three-dimensional (3D) structure as a whole tail and monomer were generated utilizing the AlphaFold2 AI DeepMind. The 3D structure of the TagX hydrolase from *A. baylyi* ADP1 was predicted by the Expasy auto-modeling software. The prepared TagX ligand was subsequently docked to the target site of selected amino acids within the Hcp1 nanotube via AutoDock Vina in Schrödinger platform. The conformational changes of the amino acid side chains upon docking were examined using RosETTAFold, and side chain rotational angles (Ψ/Φ) was detected based on the Dunbrack rotag package. The molecular docking indicated that TagX toxin binds to His 108, Arg 98, Ser 78, and Glu 121 within the Hcp1 nanotube by H-bond. This interaction induces a rotameric shift in the dihedral angles of the aforementioned amino acids initiating the contraction of the Hcp1 tail/tube via VgrG1 (gp27) contractile sheath and CLPV ATPase. This resulted in the propulsion of the effector molecule through Hcp1 to the Tip of T6SS complex and subsequent injection to prey cells.

Keywords: *Acinetobacter baumannii*, Hemolysin coregulator protein (Hcp), Artificial intelligence, AlphaFold2, Molecular docking, Amino acid rotational angle

Introduction

Gram-negative bacteria thrive in competitive environments by secreting a putative toxic effector that can kill neighboring cells [1]. They have evolved various secretory mechanisms such as the type VI secretion system (T6SS) to survive harsh conditions and eliminate competitors in mixed environments while, protecting themselves and they sister cells from inhibitory action of various effector toxins with complex cognate immunity genes (antidote), typically located upstream or downstream of the corresponding T6SS toxic effector gene [2]. T6SS, a macromolecular nanomachine, functions like a syringe and needle, injecting effectors (proteins) into neighboring cells. This process, occurring via cell-to-cell contact, is a mechanism used by bacteria to deliver toxins, compete with other microbes, and even interact with eukaryotic cells [3]. *A. baumannii* possesses a type VI secretion system which is used to kill competing bacteria, but the mechanisms and regulatory systems of its effectors are not fully understood. Specifically, the specific functions of T6SS-dependent effectors within target cells, and the regulatory systems that control T6SS expression in *A. baumannii*, require further investigation [4, 5]. The Type VI Secretion System is a bacterial weapon that allows cells to compete with each other by delivering toxins into other cells. This advantage is especially pronounced in natural environments like soil where microbial communities are diverse and resource competition is high by secretion of various putative effector molecules, including nuclease, amidase, phospholipase, peptidoglycan hydrolase, muramidase, glycosidase, NADase, and ADP-

ribosyl transferase and deliver these cytotoxins into the prey cell through by direct cell to cell contact [6, 7].

The Hcp and valine-glycine repeat protein G (VgrG) are considered the hallmarks of this secretion system, because they are secreted into the extracellular environment, thereby can be detected in the supernatants of all bacteria with functional T6SS system [8]. The crystal structure of Hcp1 protein in *A. baumannii* has been delineated by x-ray crystallography [9]. it has a tail/tube configuration with pore containing 13 putative homohexameric rings stacked on to each other constitute a 600 nm nanotube oligomer which acts both as virulence factor and has role in biofilm formation [9]. Recent structural analysis of the Hcp1 in *A. baumannii* by X-ray crystallography revealed a tight β- barrel formed by two β- sheets flanked at one side by a short α-helix and in most cases six Hcp molecules associate to form a donut-shaped hexamer [10]. The T6SS needle structure, used to deliver proteins into target cells, is assembled on a baseplate. The inner Hcp tube, which is composed of Hcp proteins, polymerizes and is wrapped by a contractile sheath composed of TssB and TssC proteins. This sheath, when it contracts, propels the Hcp tube, tipped by a spike of VgrG and PAAR proteins, through the baseplate and into a neighboring cell. The VgrG protein, and particularly the VgrG-PAAR spike, plays a crucial role in both assembly and the delivery of the effector proteins [11]. Studies of the Hcp1 proteins in Acinetobacter species using bioinformatics and X-ray tomography technique showed that, C-terminal extension toxins (Hcp-ET) is indeed exerted antibacterial properties and suppress the target cell growth when putative toxic effector bound to the inner surface [12]. T6SS-positive *A. baumannii* shows unique clinical characteristics such as increased virulence of bacteria, along with greater biofilm

formation through increase in expression of quorum sensing genes compared to T6SS-negative strains [13]. Similarly, T6SS-positive strains have a higher mortality rate in animal models and increased Hcp expression correlated well with *A. baumannii* invasiveness during respiratory infections, potentially induced by acidic conditions [14]. Furthermore, Hcp1 protein was detected in the sera of cystic fibrosis patients during *Burkholderia mallei* infecting humans or horses and function as molecular chaperone [15]. Recent report revealed that, interaction of the effector with the putative Hcp pore is a general requirement for secretion of diverse toxic effectors encompassing several putative enzymatic classes. Electron microscopy analysis of an Hcp–effector complex from *P. aeruginosa* revealed the effector bound to the inner surface of Hcp and transfer through Hcp pore to reach to needle like structure on the tip of T6SS system [16]. It is noteworthy to mention that, various bacterial species have evolved and tailored their T6SS to fulfill specific functions based on their host, ecological niche, or survival strategies. For example, the TagX peptidoglycan hydrolase from *A. baylyi* showed homology to known bacteriophage l, d-endopeptidases and its amino acid sequence was conserved in the T6SS clusters of several bacterial species [17].

This study aims to investigate the structure of the Hcp1 protein in both its individual and homohexameric forms, focusing on the conformational changes in Hcp1's ring structure when interacting with toxic effector molecules in *A. baumannii*.

1. Methods

1.1 Analysis of 3D structure of Hcp1 monomer

For the purpose of analyzing the structural and functional characteristics of the Hcp1 model, the amino acid sequence accession number WP_000653195.1 (Multispecies Acinetobacter) was retrieved from the GenBank (NBI) database and utilized as a query sequence to identify the preliminary structure, arrangements of α-helices and β-sheets, protein folding, expected position error, and degree of homology with other similar protein via a BLAST search. The sequence was then feed into different bioinformatics and artificial platforms including, SWISS-MODEL (https://swissmodel.expasy.org/), UniProtKB (https://www.uniprot.org/), a deep learning software RosETTAFold through CAMEO (https://robetta.bakerlab.org/; https://robetta.bakerlab.org/model) and AlphaFold2 (https://alphafold.ebi.ac.uk/). The sequence alignment was performed in UniProtKB database and compared with at least 5 most closely related sequences. Similarly, the secondary structures of the Hcp1 protein monomer model predicted in such way to generate the inner surface of which binds to effector molecules achieving an accuracy exceeding 90 in terms of the predicted local distance difference test (pLDDT) and predicted aligned error (PAE) values plot (http://www.subtiwiki.uni-goettingen.de/v4/pae). Finally, the quality controls for the accuracy of the predicted models were assessed using Z-score, RMSD index, B-factor, and MolProbity using Ramachandran plot. The visualization of the T6SS component structures was carried out by PyMOL through the Schrödinger platform (https://www.schrodinger.com/products/pymol). The high-quality model then selected for further experiments.

1.2 Generating the putative TagX toxic effector molecule as ligand

The putative toxic effector molecule employed here as a template was the peptidoglycan L-alanyl-D-glutamate Cwlk hydrolase (TagX) from *A. baylyi* ADP1. The amino acid sequence of the TagX protein was already reported [17] and was used to construct a three-dimensional structure of this toxic effector using Expasy automodeling server (https://swissmodel.expasy.org/interactive).

1.3. Molecular docking analysis and virtual screening

The putative TagX toxic effector protein of *A. baylyi* ADP1 was used as ligand molecule and modeled four amino acids involved in binding to effector within Hcp1 ring were consider as receptor. Molecular docking was performed using AutoDock vina in Schrödinger platform. Protein-ligand interaction complexes were visualized using PyMOL to identify binding positions of active site residues and their binding distances with Schrödinger module. The best docking poses were selected directly using the Glide by the Force field-based. The H-bonds was formed between the ligand molecule and four amino acids within Hcp1 homohexamer. This required to minimized the free energy. Here the free energy (ΔG) was minimized using GROMACS software (http://www.gromacs.org/) to create an index file with preferred dihedral angles.

1.4 Determination of Hcp1 physicochemical parameters

To evaluate the predictive properties of Hcp1 investigated in this study, we utilized the ProtParam software (https://web.expasy.org/protparam/). ProtParam is a computational tool that facilitates the calculation of various physical and chemical parameters for

proteins stored in UniProtKB or for user-entered protein sequences. The parameters computed include molecular weight, theoretical isoelectric point (pI), amino acid composition, atomic composition, extinction coefficient, estimated half-life, instability index, aliphatic index, and the grand average of hydropathicity (GRAVY).

1.5 Kapsch algorithm and the PAE plot

The goal of the Kabsch algorithm is to determine the optimal rotation matrix R that minimizes the root-mean-square deviation between two sets of points. Nevertheless, the algorithm operates in three steps: translation, computation of a covariance matrix. For further information please refer to https://pymolwiki.org/index.php/Kabsch site. Meanwhile, the PAE is useful for assessing confidence between domains or chains.

1.6 Rotamer library

An important part of this study was to determine how the toxic effector propelled from the inner membrane to the outer membrane injectosome (VgrG1 + PAAR+ Hcp1)? To answer this question, the open-source software package rotag was used to create a rotameric library using https://www.github.com/agrybauskas/rotag site. Rotag is a collection of tools that generate and analyses side-chain rotamer libraries from protein structure data. Here, to confirm the rotameric shifts or dihedral angles of the staggered amino acids within the Hcp1 monohexameric ring we used of rotamer libraries (rotag). Rotameric libraries were used to predict amino acid dihedral angle (Φ/ψ) side chains and backbone (χ1/ χ 2 and Cγ) for the possibility of rotation and protein conformation. The effect of backbone conformation on side-chain rotamer is primarily due to steric repulsion between backbone atom Cγ, whose position depends on φ and ψ side-chain heavy atoms and detected by

Ramachandran plot. One of the greatest advantages of rotag is its ability to deal with nonstandard amino acids. likewise, the current rotameric library and residue data are available at the Dunbrack website (http://dunbrack.fccc.edu/bbdep/).

1.7 Statistical analysis

All analyses were performed using SPSS, version 20 (SPSS Inc, Chicago, IL, USA). the p values were two-tailed; $p \leq 0.01$ was considered statistically significant. Means and standard deviations (SD) were calculated as required for numerical variables or unpaired t-tests were used for statistical comparisons.

2. Results

2.1. Hcp1 Homohexameric 3D Model Analysis

The cartoon illustrations of homohexamer Hcp1 from *A. baumannii* (Figure 1A) indicated that, the Hcp1 protein has multiple β-sheet barrels oriented in opposing directions, linked by short loops with the hexagonal ring. The structure generated using AlphaFold2 software revealed a tight β-barrel fold domain formed by two β sheets and one eight-residue α helix (pLDDT ≥90). Further, analysis of the of the Hcp1 homohexamer (Figure 1B) by line model, highlighted the amino acids involved in binding to the TagX toxic effector molecule arranged in interior side of Hcp1 and are situated within conserved region of the Hcp1. Indeed, the hydrophobic amino acids are buried within the Hcp1 ring while, hydrophilic amino acids are arranged in the exterior region (Figure 1B). The virtual

analysis of Hcp1 molecule also demonstrated that, the inner diameter of the Hcp1 tail/tube complex of *A. baumannii* estimated to be 40 Å, whereas the outside diameter was 80 Å arranged in the asymmetric unit. These results were supported by control measurements that assessed the accuracy of the predicted model, which included Z-score, RMSD index, B-factor, melting point, and MolProbity in the Ramachandran plot. The template demonstrated a high-quality structure with a Z-score of 1.7. The predicted alignment error (PAE) map, often used in protein structure prediction, can be compared to distance variations (DV) obtained from molecular dynamics (MD) simulations. If the PAE map shows minimal DV, it suggests a high level of agreement between the predicted structure and the dynamic behavior observed in the MD simulations. This implies that the predicted structure is a good representation of the protein's conformational landscape as determined by its PAE plot. In our case it was 5-7 scored residue (Figure 1C). At the same time, pairwise amino acid alignments of the Hcp1 protein shows conserved non-redundant region comprising putative toxic effector domain with 100% identity compare to five closely related strains obtained by UniProt database (Figure 1D). The color column and respective arrows indicates the position and kind of amino acids bind to effector molecule. Further analysis by hidden Markov model (HMM) support above results by revealing of all likelihood’s sequences for possible combinations of gaps, matches, and mismatches.

2.2. Analysis of the secondary structure of Hcp1 homohexamer

Meanwhile, to explore the number of chains of Hcp1 monomer, the schematic Spacefile structure of the Hcp1 homohexamer chains predicted in this study as demonstrated in the

Figure 2A. The presence of six chains designated as A, B, C, D, E, and F indicates that the assembly of the Hcp1 homohexamer in *A. baumannii* is a multi-complex process that necessitates additional components, such as the presence of oligomerization domain in the T6ssK protein N-terminal. Chains E and F are located on the posterior side of the hexamer. The secondary structure of Hcp1 was predicted by AlphaFold2 using PyMOL in Schrödinger platform showed the extended loop connected β2-sheet to β7 acts as a cap for the ring stabilization and interacting with the initial residues of Hcp1 (Figure 2B). Two, loops 1, and 2 in the middle of the model are helps for stability of Hcp1 from outer membrane to exterior region. Further analysis indicated that, the β6, β7, β8 and short α-helix play role in Hcp1 chaperon activity as shown by X-ray crystallography of the He et al. [21]. The important observation in this research was that, the β3, β4, β7, β8 sheets stack together to form a β- barrel with a hydrophobic core as it was detected by amino acids bond to effector. The quality and reliability of the present study model was assessed based on parameters such as pLDDT and PAE values as described in the methods. The results revealed that, the first β-plate is formed by strands β1, β4, β6, β8, are packs against the second β-sheet by strands β2, β3, β5, and β7, respectively thus forming a β-barrel fold. To find the percent angstrom-level errors in the dihedral angles of the amino acid backbone and side chains involved in binding to toxic effector, the RosETTAFold program was employed as shown in the Figure 2C. One peak error was found at position 50 in the graph signify the accuracy in amino acids residual conformation changes.

2.3. Characterization of the Toxic Effector TagX

The elimination of target cells has been observed across various species of Acinetobacter, specifically *A. nosocomialis* M2, *A. baumannii*, and *A. baylyi* ADP1. In this study, the peptidoglycan L-alanyl-D-glutamate Cwlk hydrolase, known as TagX, from *A. baylyi* ADP1 toxic effector selected as a template (Figure 3). The amino acid sequence of the TagX enzyme obtain from Weber et al. [17] paper and was employed to construct a three-dimensional structure of this toxic effector in this study. The structure of TagX effector was consisted of one α-helix linked by several loops to four small β-sheets, which were located at the N-terminal of the enzyme and two domains, one connected to the α-helix in the form of a transmembrane nexus, and the other functioning as a peptidase activity. This peptidase domain is a bacterial peptidoglycan hydrolase that cleaves the peptide bonds within the peptidoglycan matrix, leading to cell lysis. It functions similarly to *Tle*1 from *P. aeruginosa*, another peptidoglycan hydrolase that targets the same structure and causes cell death [18].

2.4. Molecular Docking and Conformational changes in the Hcp1

A key aspect of this study was to determine how the toxic effector is transported from the inner membrane to the outer membrane injectosome (VgrG1 + PAAR + Hcp1) and to neighboring cell. To address this issue, the TagX effector molecule was docked to specific amino acids within the Hcp1 monomer using AutoDock Vina within the Schrödinger platform. The docking analysis revealed that, four amino acids Arginine, Serine, Histidine and glutamic acid are playing central role in binding to TagX α- helix and β-sheet form hydrogen bonds (Fig. 4A). The estimated rotational angles of the bond amino acids showed a rotameric shifts in the dihedral angles of these four amino acids by; His (18 Å),

Arg 98 (9 & 8.6 Å), Ser 78 (13 Å), and Glu (12 Å) within the Hcp1 ring, respectively. Only in case of Arg 98 we found rotameric shift in dihedral angle of both back bone and side chain. This might be due to nature of amino acid or effector compound which effect Cβ and N bond (φ) in χ2 axis. These angles may also indirectly influence the side chains of amino acids, such as χ1 (between Cα and Cβ) and χ2 (between Cβ and Cγ). These rotameric shifts in dihedral angels of above amino acids leads to changes in the conformation of amino acids within Hcp1 so that it activates other component of T6SS like VgG29 contractile sheath and CLVP ATPase proteins and cause contraction of 600 Hcp1 nanotube. Ramachandran plot of Hcp1 monomer docked with TagX depicted in Figure 4B, whereas Cartoon depiction of amino acids on β6 and β8 strands that form H-bond with TagX effector molecule are illustrated in Figure 4C, respectively.

2.5. Prediction of the entire structure of Hcp1 by AI

The entire *A. baumannii* schematic 3D structure of the Hcp1 as well as N-terminal oligomerization domain of T6ssK protein are depicted in the Figures 5A and 5B. As Figure 5A indicate, the complete structure of the Hcp1 protein was consisted of 13 homohexamer stacked on top of each other one by one in the form of 600 nm Hcp1 nanotube through which a toxic effector TagX transported to injectosome in the Tip of T6SS. The Hcp1, a transmembrane tail/tube protein is connected to baseplate via VgrG(gp27) contractile sheath to outer membrane VgrG(gp5), and PAAR complexes. The T6SS TssB/TssC proteins are require for 600nm tail/tube stabilization form an stable injectosome. Meanwhile, the 3D structure of TssK shows it is trimeric protein containing 3 domains, one situated at N-terminal region of the protein is homologues to phage receptor binding

site and is help the oligomerization of the Hcp1 monomers, a central α- helix region and a transmembrane binding site (Fig. 5B).

2.6. T6SS prediction in *A. baumannii* by Artificial intelligence

The entire structure of the type VI secretion system in *A. baumannii* was generated using machine learning AI system (Figure 6A and 6B). These figures show the latest in silico structure prediction of T6SS report utilizing artificial intelligence. Here, the position of individual component of the system was illustrated along with complete T6SS structure. The inner membrane is composed of a baseplate containing 3-proteins complexes (T6ssK, T6ssF, T6ssG). To this complex is associated with the transmembrane proteins (T6ssL, T6ssM. T6ssJ) in form of asymmetry entity. Furthermore, TssB and TssC, forming a stable dimer that is the repeated unit for sheath polymerization (Figure 6B). Six TssB/C dimers wraps around Hcp tail/tube and stabilize 600nm Hcp1 nanotube. Effector delivered by the T6SS is loaded within the inner tube transported to the needle like spike complex and then injected to targeted prokaryotic and/or eukaryotic cells which are situated on the tip of T6SS macromolecule.

2.7. Determination of Hcp1 chemical composition and amino acids constitution

The ProtParam software was used to determine several physicochemical properties of Hcp1, including its extinction coefficient, instability index, aliphatic index, and GRAVY value. The results indicated an extinction coefficient of 39,420 $M^{-1}cm^{-1}$, an instability index of 32.86, an aliphatic index of 67.13, and a GRAVY value of -0.625. These parameters provide insights into the protein's stability, hydrophobicity, and overall characteristics (Fig. 7A). Additionally, the percent frequency of individual amino acids in

the Hcp1 structure was also estimated by same software and presented in Figure 7B. The results indicate that serine, with a frequency of 9.6%, was the most abundant amino acid, while cysteine, with a frequency of 0.6%, was the least abundant amino acid detected in this study. Tyrosine, valine, and lysine were identified as the most frequent amino acids in Hcp1 protein, respectively.

2.8. Phylogenetic tree analysis

The phylogenetic tree relationship among the Hcp1 type VI secretion system in *A. baumannii* strains was investigated as shown in Figure 8. The dendrogram was compared with closely related strains of this bacterium in the UniProtKB database. The results indicated that, the Hcp1 protein in *A. baumannii* is highly conserved with identity ≥90% with those sequence reported in UniProtKB database. It showed 100% identity with *A. baumannii* strains like A0A9P2UB1_ACIBA, A0A9Q1NHH3_ACIBA, and A9A9Q1NHH3_ACIBA, while 99.6% identity with 25 reported Hcp1 in this database (Fig. 8).

3. Discussion

While, multiple classes of Type VI Secretion System have been identified in *Acinetobacter baumannii*, they all share a fundamental similar structure and function [19]. The Hcp1 described to maintain notable structural and functional similarities to the tail of the T4 bacteriophage, indicating a potential common evolutionary lineage. This relationship not only enhances our understanding of the evolutionary dynamics underlying these biological systems but also suggests possible implications for their roles in microbial interactions and pathogenicity [20]. The structure of Hcp1 protein exhibits two β sheets

run to each other in reverse orientation and flanked at one side by a short α-helix. Six Hcp molecules associate to form a donut-shaped hexamer, as observed in both the crystal structure and solution in a symmetric orientation. Recognizing these parallels could provide valuable insights into the adaptive mechanisms employed by microorganisms, thereby affirming its significance as a critical virulence factor [10]. Majority of T6SS producing bacteria are existed in soil where there is scarcity of the presence of micronutrients among bacterial populations. Evidences suggest that they have evolved this mechanism for use as a competitive and predatory means, which was later co-opted as a mechanism for pathogen virulence [21]. Therefore, the presence of the T6SS is utmost important for survival of host cells by killing neighboring cells. The Hcp protein is both a core component of the T6SS tail tube and the exported receptor/chaperone of the effectors [22]. However, there are few information regarding the mechanism triggering contraction of the Hcp1 nanotube complex protein and how the toxic effector-Hcp1 complex was propelled into targeted cell [23].

In the present study, the changes in the dihedral angles of both the side-chain and backbone of amino acids Lys, Phe, Arg, and His within Hcp1 molecule as result of entry of TagX effector to the Hcp1 nanotube was noted. Backbone rotation is primarily due to steric repulsion between backbone atom Cγ, whose position depends on φ and ψ side-chain heavy atoms. The conformational changes were identified using RoseTTAFold AI system typically includes the specific amino acid, the corresponding dihedral angles, a measure of variance, and the likelihood of occurrence [24]. Further analysis we found that, TagX from *A. baylyi* is efficient inducer of the rotameric shift in the amino acids side-chains within Hcp1 monomer and create torsional forces and H-bound formation between

ligand molecule and receptors. This process ultimately stimulates the contraction of the Hcp1 tail/tube complex aided by VgrG1(gp27) contractile sheath and ATP hydrolysis, thereby propelling the effector molecule into the target cell. The internal pore, part of the Hcp hexamer, is capable of accommodating small, folded proteins (under 20 kDa) or unfolded proteins. This includes proteins like *Tse*1-3 from *P. aeruginosa* and *EvpC* from *Edwardsiella tarda*, which are known to bind to the inner surface of the Hcp hexamer. Specifically, the Hcp hexamer, with its β-barrel domain, forms a ring-like structure with an inner diameter of approximately 40 Angstroms. This size limitation allows for the transport of smaller proteins through the pore, while larger, folded proteins are excluded [25].

The significant contribution of this study lies in creating a three-dimensional model of the TagX effector molecule. This model is based on the amino acid sequence data reported by Weber et al. [17]. They worked revealed TagX effector molecule containing two main domains namely peptidoglycan hydrolyase which hydrolysis cell wall and cause lysis and other domain is contained transmembrane helix connected through β- sheets to long loops. Recent study indicates that in *Xanthomonas bovienii*, Hcp1 but not Hcp2 is required to suppress the prey bacterial populations. In one case it appears that mutation Arg-to-Ala at position 30 within the extended Hcp1 resulted in a significant decrease in cytotoxicity, suggesting mutations of Hcp1 shut down the functioning of all T6SS components [26, 27]. Over all the application of AI in epidemiology, microbial ecology and forensic microbiology is also outlined, underscoring its proficiency in deciphering complex microbial interactions and forecasting disease outbreaks. We critically examine the challenges in AI application, such as ensuring data quality and overcoming algorithmic

constraints, and stress the necessity for interpretable AI models that align with medical and ethical standards [28].

4. Conclusions

The study focuses on how TagX interacts with Hcp1 nanotubes, which are crucial for the delivery of toxic molecules by the T6SS (translocation system). The interaction leads to Hcp1 nanotubes contracting and propelling the effector molecule toward the tip of the injectosome (the T6SS). AlphaFold2 and bioinformatics software were used to elucidate the mechanism, revealing that TagX binding induces rotameric shifts and conformational changes in Hcp1, ultimately triggering contraction of 600 nanotube via the VgrG1 sheath, TssM, and ATP hydrolysis. This research also highlights the potential of machine learning in drug discovery by identifying a promising candidate for targeting Gram-negative pathogens.

List of Abbreviations

A. baumannii: *Acinetobacter baumannii*,

T6SS: type 6 secretion system,

Hcp: hemolysin coregulator protein,

PAAR: proline-alanine-alanine-arginine,

A2: AlphaFold2,

PAE: Predicted aligned error

Author Contributions

SHMR: Conceptualization, Data curation, Methodology. SSH: Writing original draft contributing to data mining and software analysis. All authors have read and agreed to the published version of the manuscript.

Availability of Data and Materials

The raw data supporting the conclusions of this article is made available by the authors, without undue reservation in preprint at research square site

https://www.researchsquare.com

Consent for Publication

Not applicable.

Conflicts of interest

The authors declare that no conflicts of interest exist.

Funding

No fund was used for this research.

Acknowledgements

The authors would like to thanks the staff of Research Center for Infectious Diseases and Tropical medicine, Kerman university of Medical Sciences, Iran, Medical Mycology and Bacteriology Research Center, Kerman University of Medical Sciences, Kerman, Iran, and Department of Microbiology and Virology, Kerman University of Medical Sciences for their help and computer assist in this investigation.

References

1. Le NH, Pinedo V, Lopez J, Cava F, Feldman MF. Killing of Gram-negative and Gram-positive bacteria by a bifunctional cell wall-targeting T6SS effector. Proc Natl Acad Sci U S A. 2021;118(40):e2106555118. http://doi:10.1073/pnas.2106555118.

2. Jiang X., Li H, Ma J, et al. Role of Type VI secretion system in pathogenic remodeling of host gut microbiota during *Aeromonas veronii* infection. ISME J. 2024;18(1):wrae053. https://doi:10.1093/ismejo/wrae053.

3. Yang X, Long M, Shen X. Effector Immunity Pairs Provide the T6SS Nanomachine its Offensive and Defensive Capabilities. Molecules. 2018;23(5):1009. Published 2018 Apr 26. doi:10.3390/molecules23051009

4. Carruthers MD, Nicholson PA, Tracy EN, & Munson RS. *Acinetobacter baumannii* utilizes a type VI secretion system for bacterial competition. *PloS one*. (2013) 8(3): e59388. doi.org/10.1371/journal.pone.0059388

5. Motta EVS, Lariviere PJ, Jones KR, Song Y, & Moran NA. Type VI secretion systems promote intraspecific competition and host interactions in a bee gut symbiont. *PNAS* (2024).121(44): e2414882121. doi.org/10.1073/pnas.2414882121

6. Saraswati S, Sahana R, Verma KS, Kamal M, et al. Pyrazoles: A Master Key to Tackle Multidrug-Resistant Acinetobacter baumannii and Its Structure Activity Relationship Studies. Chemistry & Biology Drug Design, 2025;105, e70092. https://doi.org/10.1111/cbdd.70092.

7. Wang T, Hu Z, Du X, et al. A type VI secretion system delivers a cell wall amidase to target bacterial competitors. Mol Microbiol. 2020;114(2):308-321. doi:10.1111/mmi.14513

8. Peng Y, Wang X, Shou J, et al. Roles of Hcp family proteins in the pathogenesis of the porcine extraintestinal pathogenic Escherichia coli type VI secretion system. Sci Rep. 2016;6:26816. Published 2016 May 27. doi:10.1038/srep26816.

9. Ruiz FM, Santillana E, Spínola-Amilibia M, Torreira E, Culebras E, Romero A. Crystal structure of Hcp from Acinetobacter baumannii: A component of the Type VI secretion system. PLoS One. (2015) 10(8):e0136978. doi:10.1371/journal.pone.0136978.

10. Ruiz FM, Lopez J, Ferrara CG, et al. Structural Characterization of TssL from *Acinetobacter baumannii*: a Key Component of the Type VI Secretion System. J Bacteriol. 2020;202(17):e00210-20. Published 2020 Aug 10. doi:10.1128/JB.00210-20

11. Silverman JM, Brunet YR, Cascales E, Mougous JD. Structure and regulation of the type VI secretion system. Annu Rev Microbiol. 2012;66:453-472. doi:10.1146/annurev-micro-121809-151619.

12. Ma J, Pan Z, Huang J, Sun M, Lu C, & Yao H. The Hcp proteins fused with diverse extended-toxin domains represent a novel pattern of antibacterial effectors in type VI secretion systems. Virulence. (2017) 8(7):1189–1202. doi.org/10.1080/21505594.2017.1279374.

13. Lin Y, Zhao D, Huang N, Liu S, Zheng J, Cao J, Zeng W, Zheng X, Wang L, Zhou T, Sun Y. Clinical impact of the type VI secretion system on clinical characteristics, virulence and prognosis of Acinetobacter baumannii during bloodstream infection. Microb. Pathog. (2023) 182:106252. doi.org/10.1016/j.micpath.2023.106252.

14. Kim J, Lee JY, Lee H, et al. Microbiological features and clinical impact of the type VI secretion system (T6SS) in Acinetobacter baumannii isolates causing bacteremia. Virulence. 2017;8(7):1378-1389. doi:10.1080/21505594.2017.1323164.

15. Ma J, Sun M, Pan Z, Song W, Lu C, Yao H. Three Hcp homologs with divergent extended loop regions exhibit different functions in avian pathogenic Escherichia coli. Emerg Microbes Infect. 2018;7(1):49. Published 2018 Mar 29. doi:10.1038/s41426-018-0042-0.

16. Li M, Le Trong I, Carl MA, et al. Structural basis for type VI secretion effector recognition by a cognate immunity protein. PLoS Pathog. 2012;8(4):e1002613. doi:10.1371/journal.ppat.1002613.

17. Weber BS, Hennon SW, Wright MS, et al. Genetic Dissection of the Type VI Secretion System in Acinetobacter and Identification of a Novel Peptidoglycan Hydrolase, TagX, Required for Its Biogenesis. mBio. 2016;7(5):e01253-16. Published 2016 Oct 11. doi:10.1128/mBio.01253-16.

18. Chou S, Bui NK, Russell AB, et al. Structure of a peptidoglycan amidase effector targeted to Gram-negative bacteria by the type VI secretion system. Cell Rep. 2012;1(6):656-664. doi:10.1016/j.celrep.2012.05.016

19. Li P, Zhang S, Wang J, et al. Uncovering the Secretion Systems of Acinetobacter baumannii: Structures and Functions in Pathogenicity and Antibiotic Resistance. Antibiotics (Basel). 2023;12(2):195. Published 2023 Jan 17. doi:10.3390/antibiotics12020195

20. Veesler D, Cambillau C. A common evolutionary origin for tailed-bacteriophage functional modules and bacterial machineries. Microbiol Mol Biol Rev. 2011;75(3):423-433. doi:10.1128/MMBR.00014-11

21. Basler M, Mekalanos JJ. Type 6 secretion dynamics within and between bacterial cells. Science. 2012;337(6096):815. doi:10.1126/science.1222901.

22. Mougous JD, Cuff ME, Raunser S, et al. A virulence locus of Pseudomonas aeruginosa encodes a protein secretion apparatus. Science. 2006;312(5779):1526-1530. doi:10.1126/science.1128393.

23. Allsopp LP, Bernal P. Killing in the name of: T6SS structure and effector diversity. Microbiology (Reading). 2023;169(7):001367. doi:10.1099/mic.0.001367

24. Meng Y, Zhang Z, Zhou C, et al. Protein structure prediction via deep learning: an in-depth review. Front Pharmacol. 2025;16:1498662. Published 2025 Apr 3. doi:10.3389/fphar.2025.1498662.

25. Zheng J, Leung KY. Dissection of a type VI secretion system in Edwardsiella tarda. Mol Microbiol. 2007;66(5):1192-1206. doi:10.1111/j.1365-2958.2007.05993.x

26. Song C, Yang B. Mutagenesis of 18 type III effectors reveals virulence function of XopZ(PXO99) in Xanthomonas oryzae pv. oryzae. Mol Plant Microbe Interact. 2010;23(7):893-902. doi:10.1094/MPMI-23-7-0893

27. Muhammad Asam Raza, Umme Farwa, Muhammad Danish, Seyhan Ozturk, et al. Computational modeling of imines based anti-oxidant and anti-esterases compounds: Synthesis, single crystal and In-vitro assessment. Computational Biology and Chemistry. 2023; 104: 107880. https://doi.org/10.1016/j.compbiolchem.2023.107880.

28. Tsitou, V. M., Rallis, D., Tsekova, M., & Yanev, N. Microbiology in the era of artificial intelligence: transforming medical and pharmaceutical microbiology. Biotechnology & Biotechnological Equipment. (2024); 38(1). 2349587 https://doi.org/10.1080/13102818.2024.2349587

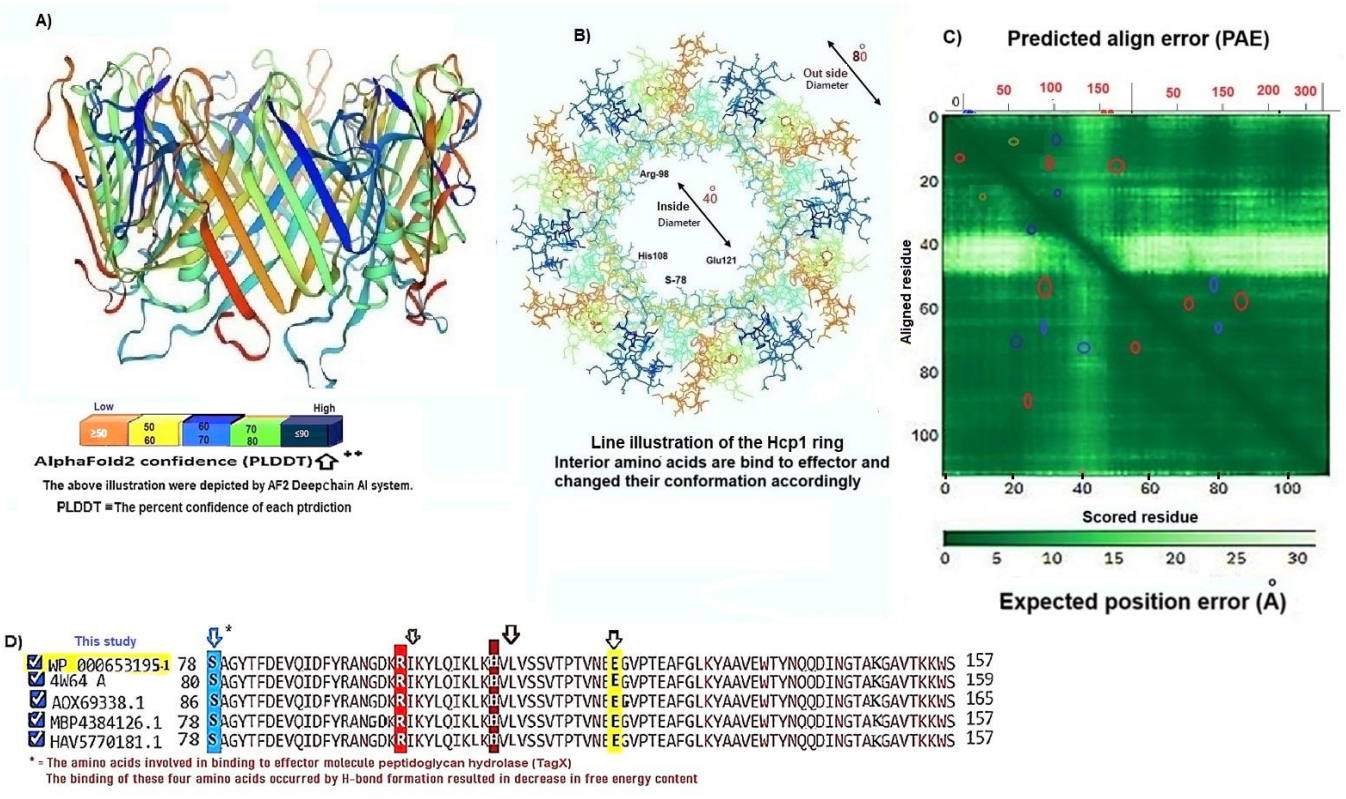

FIG. 1. (A) The cartoon representation of the three-dimensional model of the Hcp1 homohexamer in this organism, generated using the AlphaFold2 server. The structure features interconnected β-sheets, which are accentuated by small loops, alongside short α-helices that alternate with the β-sheets, resulting in a donut-shaped configuration. The β-sheets are arranged in an antiparallel orientation. The effector molecule is illustrated as a black ring located at the center of the pore. The model's reliability is indicated by a high predicted local distance difference test (PLDDT) score exceeding 90 (PLDDT>90). (B) A line model representation of the Hcp1 ring, highlighting the amino acids involved in docking with the effector molecule. The molecular dynamic model, derived from AlphaFold2, has been validated by Expasy Swiss-Prot and is based on the *A. baumannii* 4w64.3 template. (C) The predicted alignment error (PAE) measured in Angstroms for the Hcp1 monomer discussed in this analysis was calculated using a modified Kabsch algorithm in conjunction with the deep learning-based RosETTAFold program. The resulting plot illustrates a prominent peak of error at residue 50. (D) Multiple amino acid sequence alignments (MSAs) for four closely related strains of *A. baumannii*, showcasing the highest identity within the consensus sequence, were executed with Clustal Omega (www.clustal.org). The amino acids implicated in binding to the effector molecule are highlighted with colored arrows.

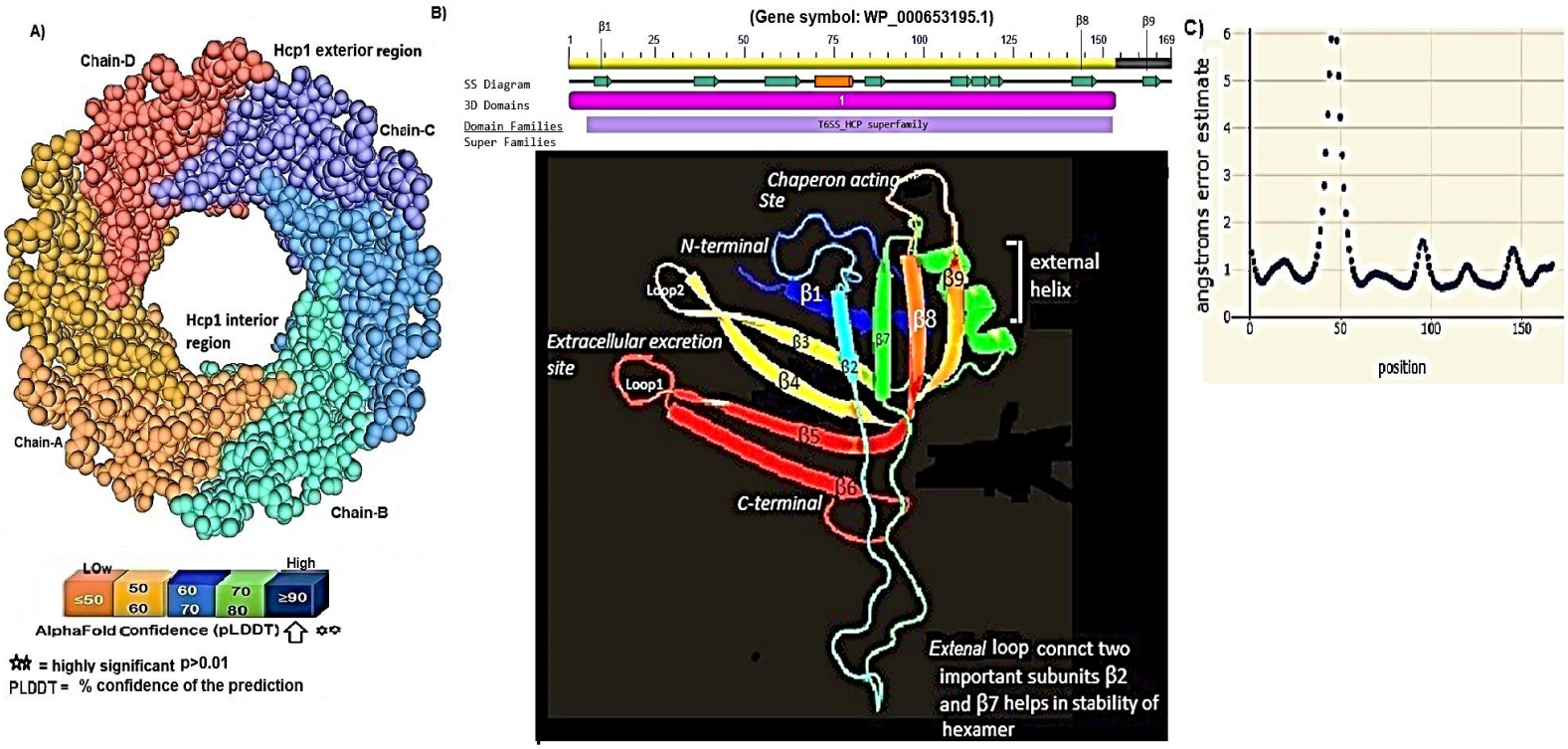

FIG. 2. Predictions related to Hcp1 chains and their functional binding sites are this figure. (A) This section presents the Spacefile predictions for the Hcp1 chains within the T6SS system of *A. baumannii*. The illustration demonstrates the identification of six distinct chains labeled A, B, C, D, E, and F, indicating that the assembly of the Hcp1 homohexamer in A. baumannii is a complex multi-component process. This process requires supplementary elements, including the N-terminal domain of the T6ssK proteins, which play a crucial role in the functioning of Hcp1. Notably, chains E and F are situated on the posterior aspect of the hexamer. (B) The modeling of the Hcp1 monohexamer was executed utilizing PyMOL on the Schrödinger platform, revealing a structure characterized by eight β-strands that create a compact β-barrel, alongside a singular α-helix and an extended loop. These structural predictions stem from AlphaFold2 (AF2) analyses and were visualized through PyMOL within the Schrödinger framework. (C) A depiction of the alterations in angstrom error related to the dihedral angles of amino acid side chains and their configurations that are essential for binding to the effector molecule. The conformational adjustments were examined using the RosETTAFold program, which employs deep learning AI technology. The peak observed in the graph signifies fluctuations in dihedral angles at position 50 upon effector binding, providing an estimation of the model's minimum error.

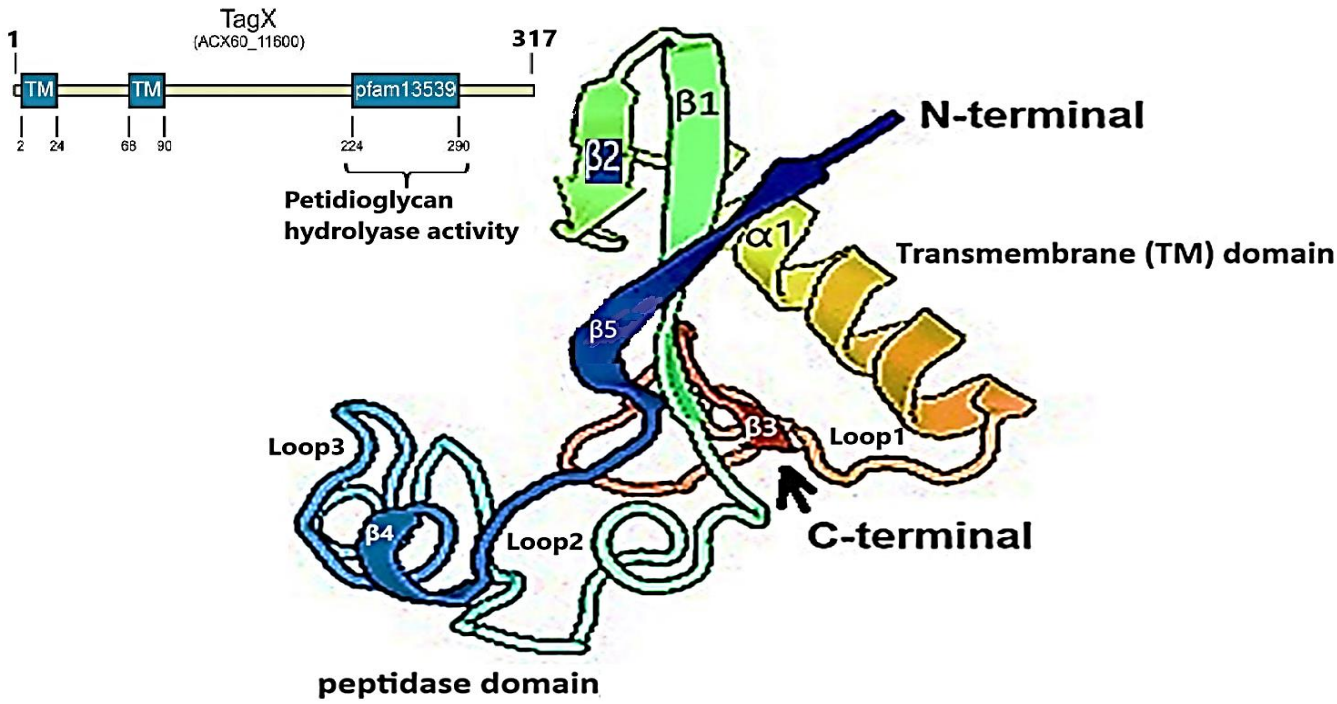

3D structure and domain analysis of the TagX putative toxic effector investigated in this study utilizing AlphaFOLD2 program

gyelvllegyrspeqqnllsgnpnt·····trargyqsyhqlglaadva·fkrngkvviserdpwamrgyqllygeva··esvgltwggrwksiqdyghte

Template: A. baylyi ADP1 TagX 198-289 region

Function A Peptidoglycan L-alanyl-D-glutamate endopeptidase CwlK

The sequence was obtained from following reference: Weber, B. S., S. W. Hennon, M.S. Wright, et al. 2016. Genetic dissection of the Type VI Secretion System in Acinetobacter and identification of a novel peptidoglycan hydrolase, TagX, required for its biogenesis.mBio 7(5): e01253-16.

FIG. 3. The schematic representation and amino acid composition and residues of the primary domains of TagX peptidoglycan hydrolyase (pfam13539) are outlined. The structure feature contains an α-helix that functions as a transmembrane domain, which is linked to four β-sheet barrels via multiple loops. The β-sheets are responsible for the endopeptidase activity observed in this enzyme. Notably, the β3 sheet is located at the C-terminal end of the protein. The structural model of this toxin was developed using AlphaFold2, with *A. baylyi* ADP1 serving as the template organism. The model alignment demonstrated a pLDDT value of 90 or higher. The amino acid sequence for the TagX effector was sourced from the work of Weber et al. (2016) [17].

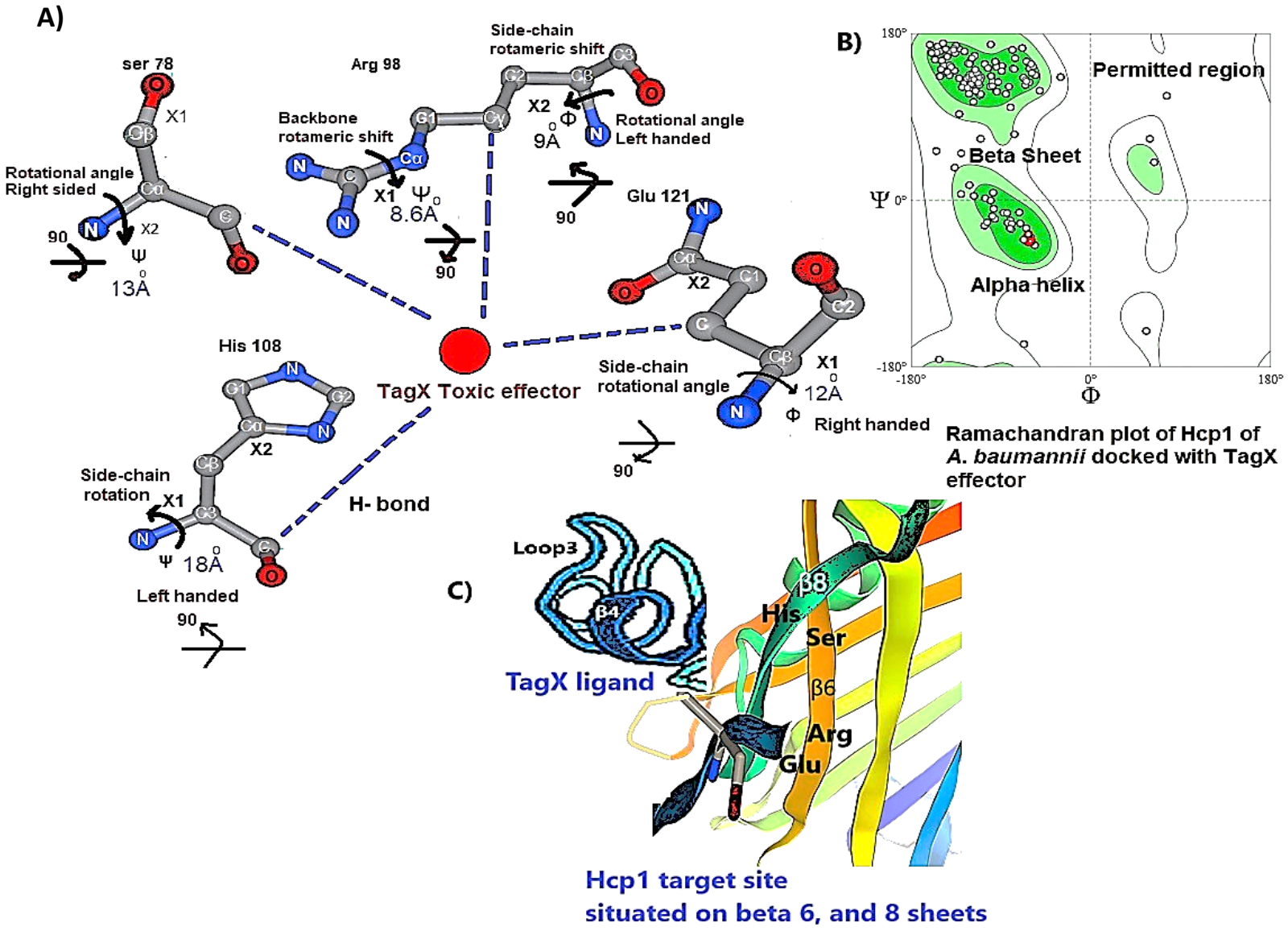

FIG. 4. Molecular docking of four amino acids with putative TagX effector. Molecular docking was conducted on four amino acids—His 103, Ser 71, Arg 89, and Glu 121- of the Hcp1 nanotube in interaction with the putative TagX effector, focusing on hydrogen bond formations. The rotameric shifts in dihedral angles are indicated by arrows. Notably, for Arginine, the rotational angles φ and ψ were observed to change in both the backbone and side chain of the amino acids. The docking analysis utilized AutoDock Vina, and the pose with the highest quality, exhibiting a Z-score of 1.7, was selected as the ligand.

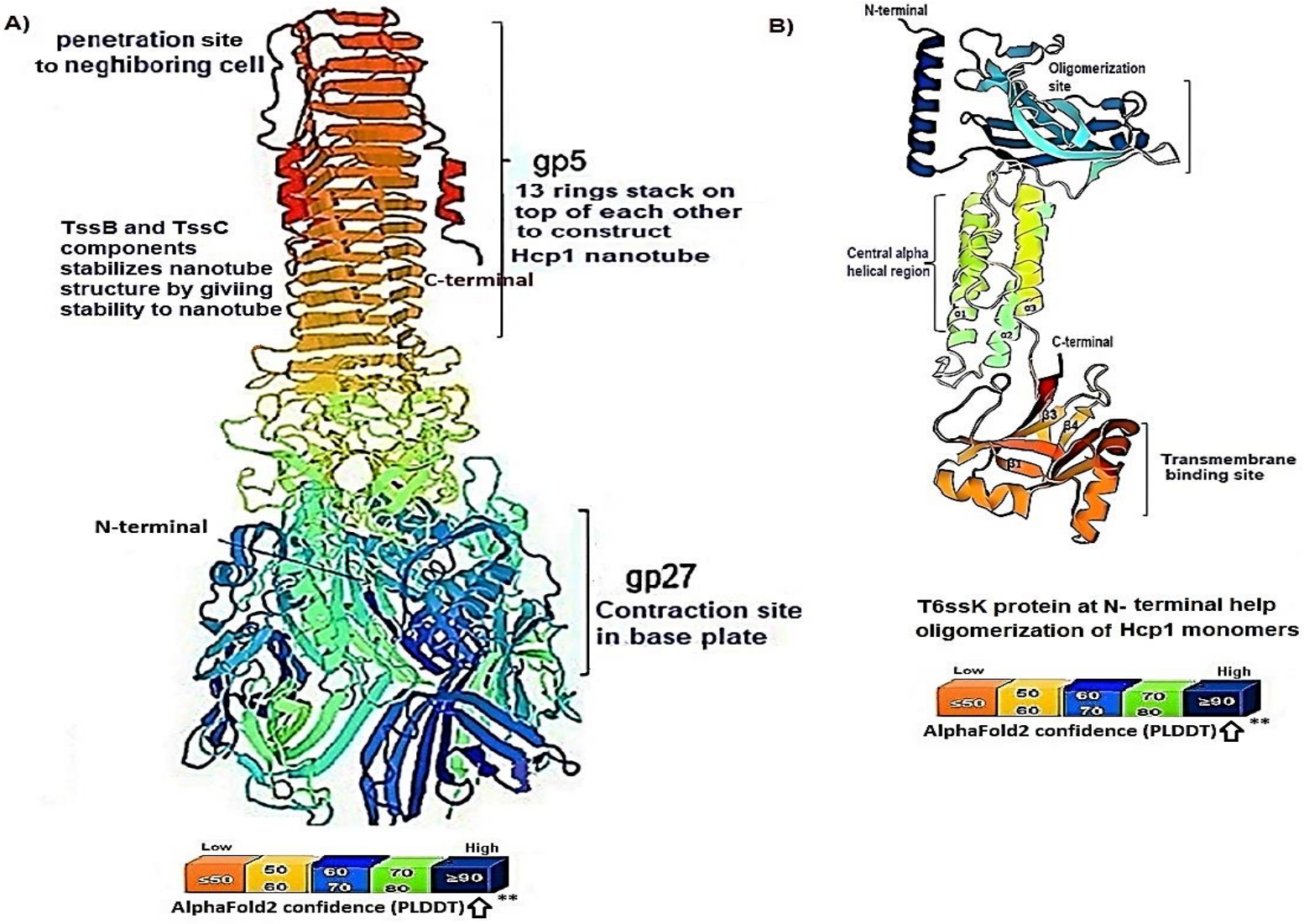

FIG. 5. The whole structure of the Hcp1 oligomer in *A. baumannii* depicted in this study by alfafold2 software. (A)The schematic representation of the Hcp1 tail/tube complexes in *A. baumannii*; i) domain-1 features at the C-terminal of VgrG1 (gp5) functioning as needle, attached to the upper part of Hcp1 ii) domain-2 comprises 13 homohexamers stacked on each other to form of 600nm tubule's contractile structure, the T6ssB/C proteins play role in stability of Hcp1 oligomer, h iii) The depicted structure Domain-3 consisting of VgrG1 (27) contractile sheath attached noncovalently to base plate. (B) The schematic representation of T6ssK protein N- terminal domain consist of amino acids residues require for Hcp1 oligomerization.

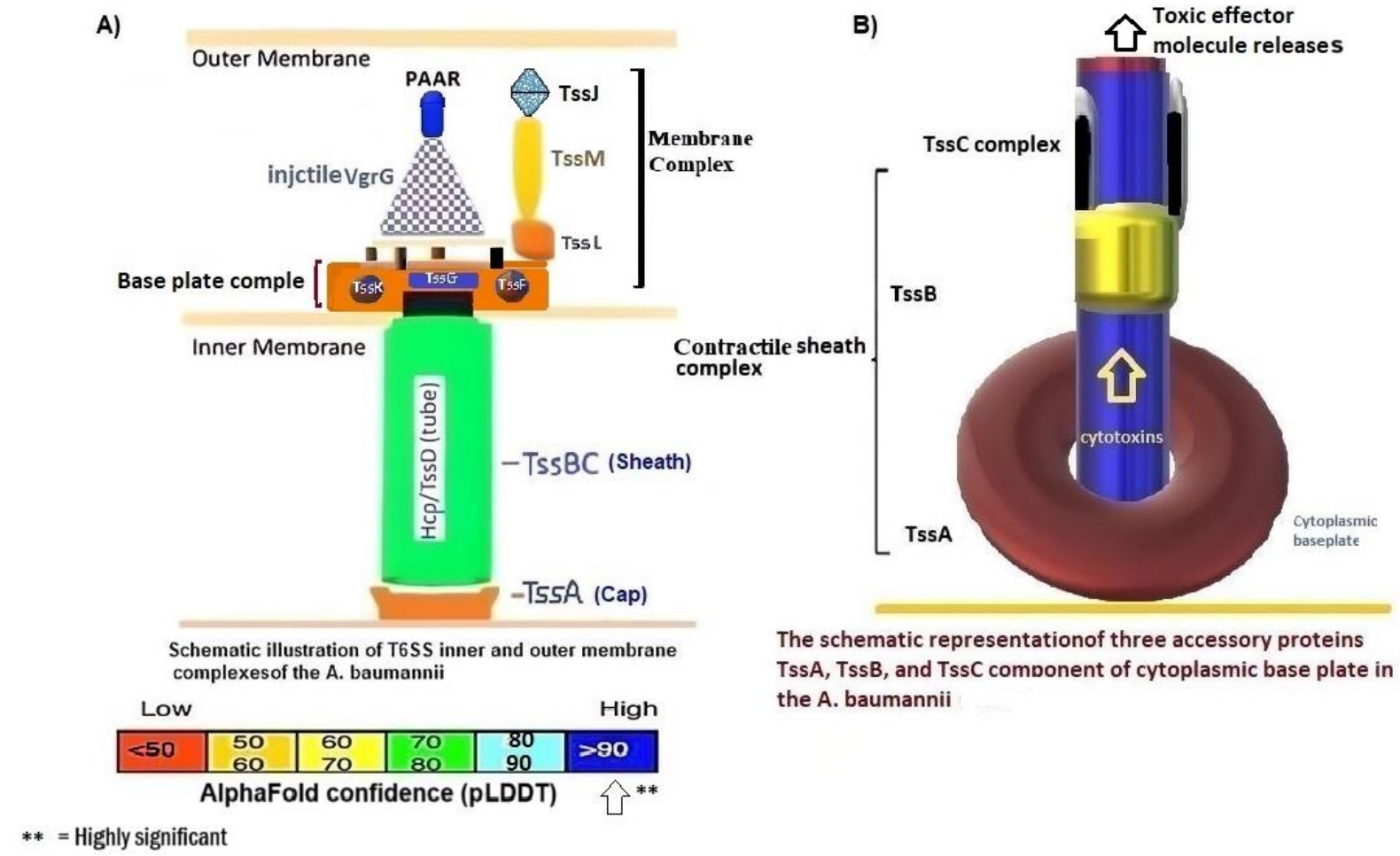

FIG. 6. This figure illustrates the comprehensive architecture of the type VI secretion system (T6SS) in *A. baumannii* through artificial intelligence system using both neural deep learning and DeepMind methodology. (A) The overall configuration of the T6SS in *A. baumannii*, reveals that the inner membrane complex comprises a baseplate formed by the proteins TssK, TssF, TssG, and TssE. Additionally, the Hcp1 tail/tube complex connected to VrgG1(gp27) at baseplate to periplasmic space serves as a pivotal element of the T6SS, playing a crucial role in the delivery of effector molecules to target cells. The base plate is anchored to the outer membrane through a complex of three proteins: TssM, TssL, and TssJ, with TssJ specifically interacting with the cell membrane lipoprotein. The injectosome is characterized by three needle-like structures known as VgrG1 (gp5) and includes a PAAR domain. (B) The contractile sheath complexes containing TssB/C proteins covered the Hcp1 nanotube, which causes stability of the oligomer, while TssA facilitating this connection. The cytotoxins are transported through 20 angstrom pore at the inner membrane as shown in arrow to outer membrane. The proteins of outer membrane have transmembrane activity majority possess domains with long α-helices. It the pass to Hcp1 + VgrG1 (gp5) and PAAR and injected into prey cell. Each of these proteins containing effector binding cargo site.

A)

```
        10         20         30         40         50         60
MKDIYVEFRG KYKVDGESRD SEHKGWLEVN SWSHNIRQPK SATSSSVGGH TAERVEHSDM

        70         80         90        100        110        120
VFVKDLDATS PKLWEACSAG YTFDEVQIDF YRANGDKRIK YLQIKLKHVL VSSVTPTVNE

       130        140        150        160
EGVPTEAFGL KYAAVEWTYN QQDINGTAKG AVTKKWSLSN NTASYAA
```

Total number of negatively charged residues (Asp + Glu): 22
Total number of positively charged residues (Arg + Lys): 21

Atomic composition:

Carbon	C	833
Hydrogen	H	1278
Nitrogen	N	228
Oxygen	O	260
Sulfur	S	3

Formula: C833H1278N228O260S3
Total number of atoms: 2602
Extinction coefficients:
Extinction coefficients are in units of M-1 cm-1, at 280 nm measured in water.
Ext. coefficient 39420
Abs 0.1% (=1 g/l) 2.103, assuming all pairs of Cys residues form cystines
Estimated half-life:
The N-terminal of the sequence considered is M (Met).
The estimated half-life: 30 hours (mammalian reticulocytes, in vitro).
>20 hours (yeast, in vivo).
>10 hours (Escherichia coli, in vivo).
Instability index:
The instability index (II) is computed to be 32.86
This classifies the protein as stable.
Aliphatic index: 67.13
Grand average of hydropathicity (GRAVY):-0.625

B)

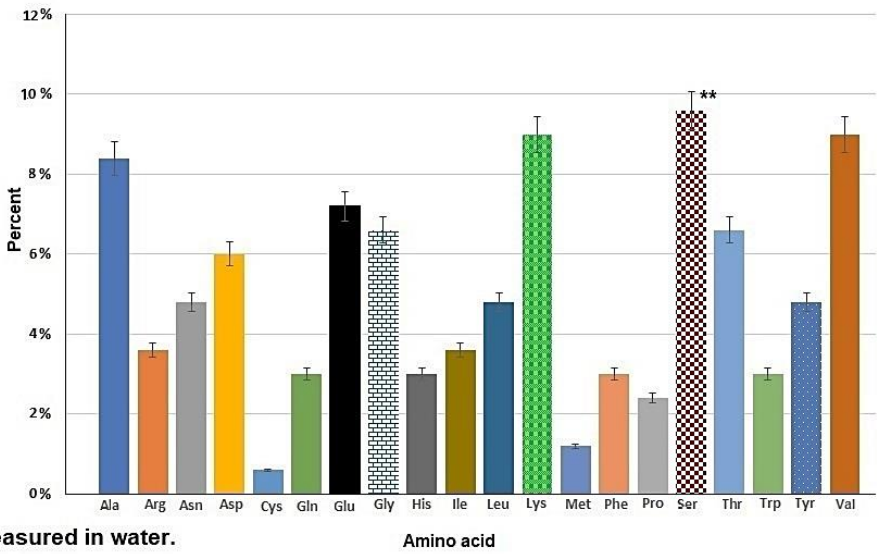

The error bars indicate the SD representing the means from three independent experiments. **, P < 0.01.

FIG. 7. The physicochemical properties of Hcp1, along with the amino acid composition in the hospital strain of *A. baumannii*, are examined in detail. (A) The characteristics encompass atomic composition, total atom count, extinction coefficient, estimated half-life, and the molecular weight of the protein. (B) In a similar manner, the amino acid composition is represented graphically by bars, with error bars denoting the standard deviation derived from two experimental trials. Notably, serine constitutes the most abundant amino acid in the Hcp1 protein structure at 9.7%, while cysteine is the least prevalent, accounting for only 0.6%. Source (ProtParam software)

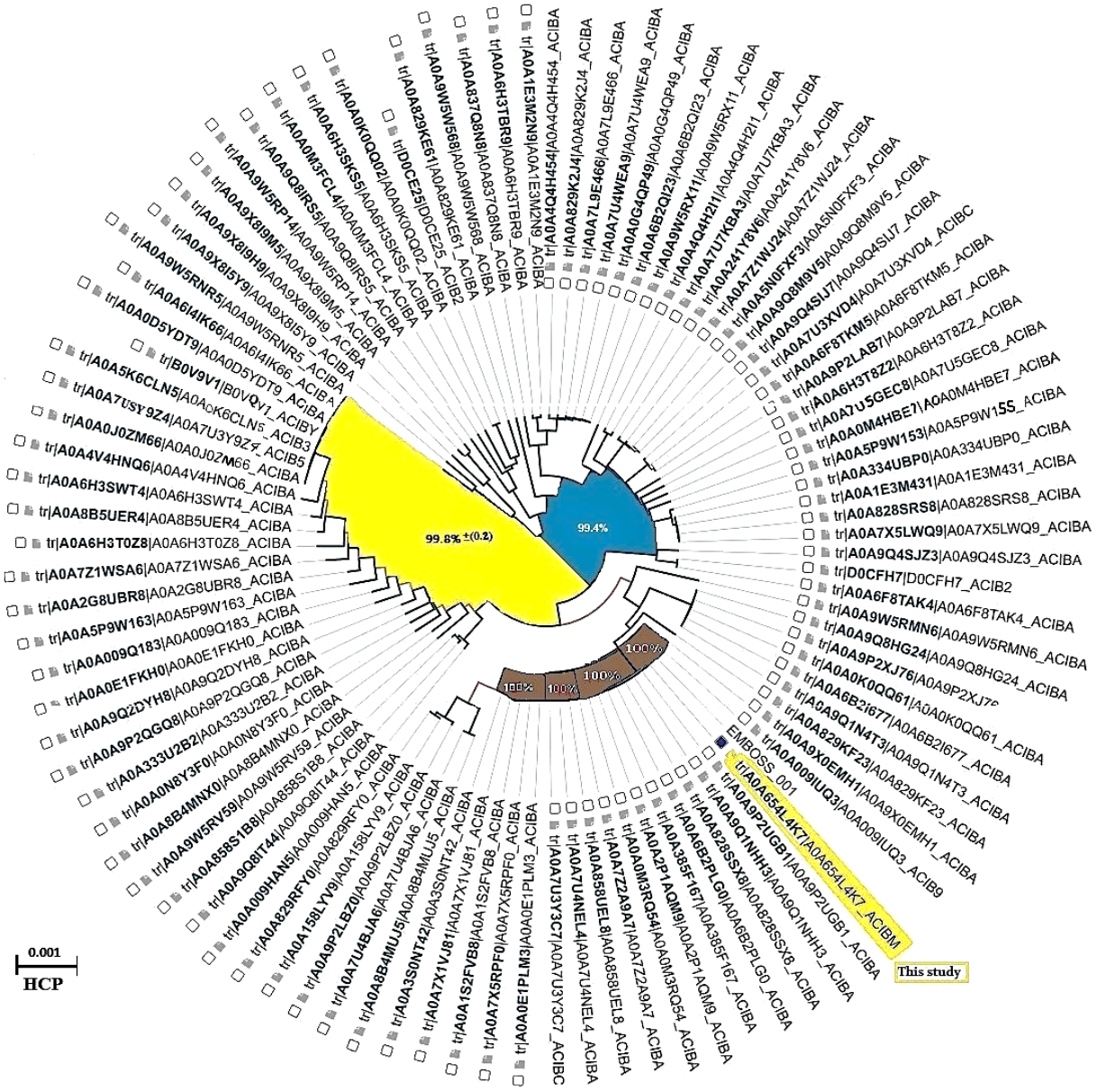

FIG. 8. This Illustration show the phylogenetic tree of the Hcp1 protein from closely related hospital strains of A. baumannii. This analysis delineates the phylogenetic relationships among the Hcp components of the Type VI secretion system (T6SS) in A. baumannii. The dendrogram was constructed utilizing the BioPython 1.58 Align package (https://biopython.org), incorporating the AlignIO and AlignInfo modules. The AlignIO module facilitates the reading and writing of sequence alignments across various formats, while the AlignInfo module provides tools for summarizing and analyzing alignment data.

The figure reveals a high degree of identity among the examined strains. Notably, four Hcp1 sequences from A. baumannii strains exhibited 100% identity with the query sequence utilized in this study, while the remaining sequences demonstrated homology exceeding 90%, as determined by the neighbor-joining method. This finding was corroborated by data from the UniProtKB database.